The *Plasmodium* eukaryotic initiation factor-2α kinase IK2 controls the latency of sporozoites in the mosquito salivary glands

Min Zhang,[1] Clare Fennell,[3] Lisa Ranford-Cartwright,[4] Ramanavelan Sakthivel,[5] Pascale Gueirard,[6] Stephan Meister,[7,8] Anat Caspi,[9] Christian Doerig,[3] Ruth S. Nussenzweig,[1,2] Renu Tuteja,[10] William J. Sullivan, Jr.,[11] David S. Roos,[9] Beatriz M.A. Fontoura,[5] Robert Ménard,[6] Elizabeth A. Winzeler,[7,8] and Victor Nussenzweig[1]

[1]Michael Heidelberger Division, Department of Pathology, [2]Department of Medical and Molecular Parasitology, New York University School of Medicine, New York, NY 10016
[3]INSERM U609, Wellcome Centre for Molecular Parasitology, University of Glasgow, Glasgow, G12 8TA, Scotland, UK
[4]Division of Infection and Immunity, Faculty of Biomedical and Life Sciences, University of Glasgow, Glasgow, G12 8QQ, Scotland, UK
[5]Department of Cell Biology, University of Texas Southwestern Medical Center, Dallas, TX 75390
[6]Institut Pasteur, Unité de Biologie et Génétique du Paludisme, Paris 75015, France
[7]Genomics Institute of the Novartis Research Foundation, San Diego, CA 92121
[8]Department of Cell Biology, The Scripps Research Institute, La Jolla, CA 92037
[9]304B Carolyn Lynch Laboratories, Department of Biology, University of Pennsylvania, Philadelphia, PA 19104
[10]Malaria Group, International Centre for Genetic Engineering and Biotechnology, New Delhi 110067, India
[11]Department of Pharmacology and Toxicology, Indiana University School of Medicine, Indianapolis, IN 46202

Sporozoites, the invasive form of malaria parasites transmitted by mosquitoes, are quiescent while in the insect salivary glands. Sporozoites only differentiate inside of the hepatocytes of the mammalian host. We show that sporozoite latency is an active process controlled by a eukaryotic initiation factor-2α (eIF2α) kinase (IK2) and a phosphatase. IK2 activity is dominant in salivary gland sporozoites, leading to an inhibition of translation and accumulation of stalled mRNAs into granules. When sporozoites are injected into the mammalian host, an eIF2α phosphatase removes the PO4 from eIF2α-P, and the repression of translation is alleviated to permit their transformation into liver stages. In *IK2* knockout sporozoites, eIF2α is not phosphorylated and the parasites transform prematurely into liver stages and lose their infectivity. Thus, to complete their life cycle, *Plasmodium* sporozoites exploit the mechanism that regulates stress responses in eukaryotic cells.

The Journal of Experimental Medicine

CORRESPONDENCE
Victor Nussenzweig:
Victor.Nussenzweig@nyumc.org

Abbreviations used: CSP, circumsporozoite protein; EEF, exoerythrocytic form; eIF2α, eukaryotic initiation factor 2α; GO, gene ontology; IMC, inner membrane complex; PABP, polyA-binding protein; TEM, transmission electron microscopy.

During initiation of protein synthesis, a ternary complex of Met-tRNA, GTP, and the eukaryotic initiation factor 2 (eIF2) is delivered to the translation initiation machinery. During this translation process, eIF2-GTP is hydrolyzed to eIF2-GDP and released from the machinery. A guanine nucleotide exchange factor (eIF2B) facilitates the exchange of eIF2-GDP to eIF2-GTP, which is a requisite for a new round of translation. The phosphorylation of eIF2α blocks the recycling of eIF2-GTP and downregulates protein synthesis (Van Der Kelen et al., 2009). This mechanism is used by mammalian cells in response to stress, thereby reducing metabolic needs and providing cells with time to recover from injury (Proud, 2005). Four different eIF2α kinases are used by vertebrates to respond to specific stresses: PEKR responds to protein misfolding in the endoplasmic reticulum, GCN2 responds to nutrient depletion, PKR responds to viral infection, and HRI responds to oxidative stress during erythrocyte maturation. The phosphorylation of eIF2α is associated with the appearance of stress granules in the cytoplasm of stressed cells. Stress granules are nonmembranous structures ranging in size from 0.1–2.0 μm that are comprised

The Rockefeller University Press $30.00
J. Exp. Med.
www.jem.org/cgi/doi/10.1084/jem.20091975

of aggregates of nontranslating mRNAs and initiation factors of translation, such as phosphorylated eIF2α, eIF3, eIF4E, eIF4G, and polyA-binding protein (PABP). The nontranslating ribonucleoproteins in stress granules are in dynamic equilibrium with the translational pool, allowing rapid shifts between translation and storage (Kedersha and Anderson, 2007; Balagopal and Parker 2009).

The response to stress via phosphorylation of eIF2α is conserved among eukaryotes, including in protozoan parasites. When *Toxoplasma gondii* tachyzoites, the rapidly multiplying forms of the parasite, are subjected in vitro to heat shock, alkaline pH, or other forms of stress, they phosphorylate eIF2α and start expressing cyst wall antigens of bradyzoites, the parasite's latent forms. These changes are associated with an arrest in translation. The inhibition of eIF2α dephosphorylation by salubrinal, a specific inhibitor of the eIF2α-P phosphatases (Boyce et al. 2005), enhances transcription of bradyzoite genes, implying that the tachyzoite/bradyzoite transformation is regulated by a yet to be identified phosphatase (Sullivan et al., 2004; Narasimhan et al., 2008).

Malaria parasites have an asexual cycle in the blood of mammals, and a sexual cycle in *Anopheles* mosquitoes. During the erythrocytic cycle, male and female gametocytes are generated and taken up by mosquitoes. Fertilization and zygote formation take place in the mosquito stomach, and the zygote develops into a motile form, named ookinete, that penetrates in the midgut epithelium and forms oocysts. Hundreds of sporozoites are generated inside a single oocyst. The mature sporozoites exit the oocysts and invade the salivary glands. After delivery to the skin of the host during mosquito bite, the salivary gland sporozoites traverse skin cells, enter the circulation, migrate rapidly to the liver, and infect hepatocytes. A new replication cycle takes place generating thousands of merozoites that exit hepatocytes, enter the blood, and invade erythrocytes.

Plasmodium sporozoites in mosquitoes are adapted for long-term survival in the salivary glands without significantly changing their transcriptional program, while maintaining their infectivity (Boyd et al., 1936; Porter et al., 1954; Sherman, 1998). This is in contrast to the continuous transcriptional changes observed in the blood and liver stages in the mammalian host and in the mosquito vector. Notably, several genes required for the development of the liver stages (also called exoerythrocytic forms [EEFs]) are transcribed, but not translated, in salivary gland sporozoites (Florens et al., 2002; Le Roch et al., 2003; Lasonder et al., 2008). In this paper, the arrested development of salivary gland sporozoites is called latency.

Three eIF2α kinases, IK1, IK2, and PK4, have been identified in *Plasmodium* (Ward et al., 2004), and their catalytic subdomains are homologous to those of other members of the eukaryotic eIF2α kinases (Fig. S1). PK4 is expressed in blood stages. Its function is unknown, but attempts to target *PK4* in *P. berghei* and *P. falciparum* have failed (unpublished data), suggesting that it is an essential gene for blood stages. The disruption of *PfeIK1* does not affect the development of the parasites in the blood of the mammalian host or in the mosquito vector. PfeIK1 function is similar to that of GCN2; it regulates the stress response of blood-stage parasites to amino acid starvation (Fennell et al., 2009). In this paper, we provide direct evidence that latency of malaria parasites in mosquito salivary glands is controlled by IK2.

RESULTS

Gene targeting of *IK2*

To determine the transcript levels of *IK2* throughout the parasite's life cycle, real-time RT-PCR was performed with cDNA from different stages of *P. berghei*. *IK2* is predominantly transcribed in salivary gland sporozoites. A significant level of *IK2* transcript is also present in gametocytes. *IK2* transcription is barely detected in the midgut sporozoites or in blood stages. *IK1* and *PK4* are mostly transcribed in the asexual blood stages (Fig. 1).

To test the function of IK2 in *P. berghei*, *PbeIK2* was replaced by double-crossover homologous recombination by the hDHFR selectable marker and a constitutively expressed GFP cassette [(*PbeIK2* (-)] (Fig. S2 A). Recombinant parasites were selected, two clones (from a single transformation) were obtained, and their disrupted *IK2* locus was verified by PCR (Fig. S2 B) and Southern blot (Fig. S2 C) analysis of parasite genomic DNA. The development of the mutants in the blood of mice, and in *Anopheles stephensi* mosquitoes, was not significantly different from that of wild-type parasites (Fig. 2, A and B). The in vitro release of *P. berghei* sporozoites from the salivary glands of wild-type and mutants did not differ significantly (Fig. 2 C). We also disrupted the *P. falciparum* orthologous gene *PfeIK2* by single-crossover homologous recombination (Fig. S3). Clones of *PfeIK2* (-) completed the sexual development in mosquitoes and invaded the salivary glands in numbers similar to wild-type (Table S1). Therefore, neither in *P. berghei* nor in *P. falciparum* IK2 is required for *Plasmodium* development in erythrocytes and in the mosquito vector.

We then tested the infectivity of *PbeIK2* (-) salivary gland sporozoites to the mammalian host by intravenous injection or via mosquito bite into mice and assessing the emergence of erythrocytic stages. After either delivery route, the infectivity of the *PbeIK2* (-) salivary gland sporozoites to mice was

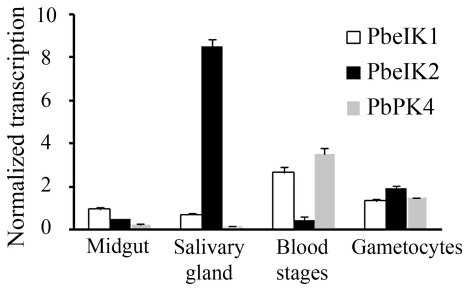

Figure 1. Stage-specific transcription of the PbeIF2α kinases. PbeIF2α kinases (PbeIK1, PbeIK2, and PbPK4) transcript levels were analyzed by real-time PCR using cDNAs from different stages of *P. berghei*. Each value is the mean ± SD of two independent experiments.

almost abolished (Fig. 2 D and Table I). The *PbeIK2* (-) salivary gland sporozoites were also defective in their ability to traverse cells (Mota et al., 2001; Fig. S4 A) and glide on glass slides (Vanderberg, 1974; Fig. S4 B), but paradoxically they invaded and developed inside of HepG2 cells with the same efficiency as wild-type (Fig. 2 E; see Discussion). We conclude that the targeting of the *IK2* does not affect parasite development in the blood stages nor in mosquitoes, but profoundly impairs the development of *PbeIK2* (-) salivary gland sporozoites in mice. The phenotype of the mutant *falciparum* sporozoites in the mammalian host was not examined because these parasites only complete their development in humans or chimpanzees.

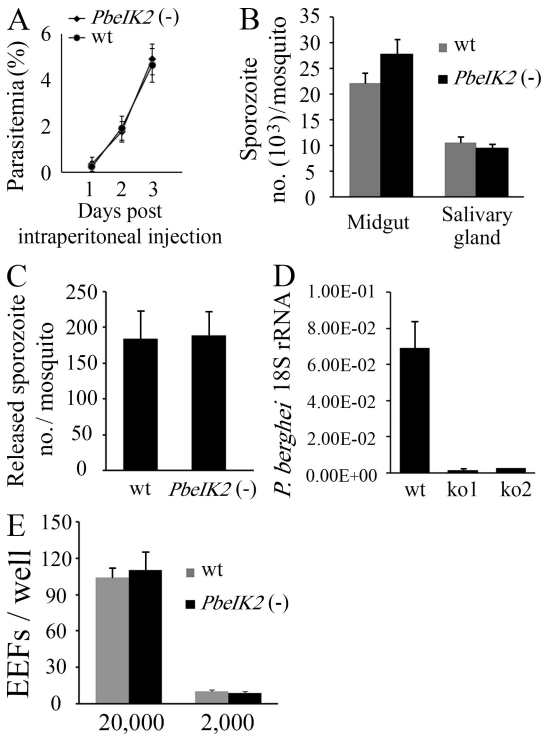

Figure 2. Phenotype of *PbeIK2* (-) sporozoites. (A) *PbeIK2* (-) parasites develop normally in asexual blood stages. Swiss Webster mice (5 per group) were injected intraperitoneally with 200 µl of blood infected with *PbeIK2* (-) or wild-type parasites (1% parasitemia). The parasitemia of the recipient mice was checked in Giemsa-stained blood smears. (B) *PbeIK2* (-) and wild-type parasites produce the same number of midgut and salivary gland–associated sporozoites on day 14 and 20 after the first infectious blood meal, respectively. Sporozoite numbers were counted in three different mosquito cycles of the wild type and mutants. (C) *PbeIK2* (-), and wild-type–infected mosquitoes release saliva containing the same number of sporozoites into the medium. Sporozoite numbers were counted in three independent experiments. (D) C57BL/6 mice (five mice per group) were intravenously injected with 1×10^4 wild type or either one of two clones of *PbeIK2* (-) sporozoites (ko1 and ko2). Liver-stage parasite burden was measured by real-time RT-PCR, and shown are the means ± SD of two independent experiments. (E) In three independent experiments 2×10^4 or 2×10^3 wild-type and *PbeIK2* (-) sporozoites were added to HepG2 cells. Infectivity of sporozoites to HepG2 cells were evaluated by counting EEF numbers 48 h after infection.

eIF2α phosphorylation in salivary gland sporozoites is mediated by IK2

We then assessed *Plasmodium* eIF2α phosphorylation in wild-type sporozoites. For this, we used a rabbit antibody raised against a peptide of *Toxoplasma* eIF2α, MSDERLpSKRRFRS, in which pS represents the phosphorylated serine (Narasimhan et al., 2008). The amino acids surrounding pS are identical between *Toxoplasma* and *Plasmodium* eIF2α, but differ from those in mammalian eIF2α. Western blot analysis of extracts of wild-type sporozoites collected from mosquito midgut, hemocoel, or salivary glands showed that although total amounts of PbeIF2α were similar in all sporozoite populations, the phosphorylation of PbeIF2α increased only in salivary gland sporozoites (Fig. 3 A). This is in agreement with the increased transcription of the *IK2* gene specifically in salivary gland sporozoites. As expected, eIF2α was not phosphorylated in the *PbeIK2* (-) sporozoites (Fig. 3 B). We conclude that PbeIF2α is phosphorylated in salivary gland sporozoites, and that PbeIF2α phosphorylation is mediated exclusively by the kinase *PbeIK2*.

Comparing protein translation in wild-type and *PbeIK2* (-) sporozoites

To study the effect of eIF2α phosphorylation on protein translation, we incorporated ^{35}S-labeled methionine and cysteine in wild-type and *PbeIK2* (-) salivary gland sporozoites for 30 min at 37°C. Salivary glands of noninfected mosquitoes, serving as control, were processed the same way. The radioautography of SDS-PAGE showed that the overall protein synthesis was greatly enhanced in the *PbeIK2* (-) (Fig. 3 C). This was expected because protein synthesis is inhibited by phosphorylation of eIF2α. The kinetics of incorporation in wild-type and *PbeIK2* (-) sporozoites was greater at 37°C than at room temperature, that is closer to the temperature of *Plasmodium* growth in mosquitoes (Fig. 3 D). Importantly, protein synthesis was greatly enhanced at both temperatures in *PbeIK2* (-).

The stalled mRNAs in salivary gland sporozoites accumulate in RNA granules

Next, we searched for the presence of stress granules in wild-type sporozoites using two methods: in situ hybridization with oligo-d(T) to detect all of the cellular poly(A)RNA, and specific staining with antibodies to PABP and phosphorylated eIF2α, which are exclusively found in stress granules. PABP is a poly(A)-binding protein that binds to poly(A) tails of mRNA and regulates mRNA stability and protein translation. These two proteins are not present in processing bodies (P bodies), another class of RNA granules that accumulate mRNA targeted for degradation (Kedersha and Anderson, 2007). As shown in Fig. 4, both assays revealed the presence of the granules in most or all wild-type parasites. PABP and phosphorylated eIF2α were not concentrated in granules in the control *PbeIK2* (-) parasites. With few exceptions, the levels of bulk poly(A) RNA were also severely decreased in the mutants. In conclusion, these experiments provide direct evidence that the presence of

Table I. Loss of infectivity of *PbeIK2* (-) sporozoites in C57BL/6 mice

Infected by		Wild type		*PbeIK2* (-)	
		Infected/total	PPDs (no. of mice)	Infected/total	PPDs (no. of mice)
Mosquito bite[a]		6 / 6	3 (6)	0 / 6	
		6 / 6	3 (6)	1 / 16	7(1)
Intravenous injection	10,000[b]	12 / 12	3(12)	5 / 12	7(2), 8(3)
	1,000[b]	6 / 6	4(6)	0 / 6	

Pre-patent day (PPD), Number of days after sporozoite inoculation until detection of erythrocytic stages by microscopic examination of blood smears.
[a]10 infected mosquitoes per mouse. Shown are results of two independent experiments.
[b]No. of injected sporozoites.

stress granules in salivary gland sporozoites is regulated by PbeIK2-mediated eIF2α phosphorylation.

Mechanisms of the loss of infectivity in the *PbeIK2* (-)

We compared the transcriptional profile of wild-type and *PbeIK2* (-) salivary gland sporozoites using microarrays (Affymetrix, containing both *P. falciparum* and *P. berghei* gene probes). The experiment confirmed the absence of *PbeIK2* transcripts in the mutant. More importantly, it also revealed that 816 out of a total of 10,734 *P. berghei* probe sets were up-regulated by more than twofold in the mutant. The microarray data were validated by real-time RT-PCR analysis of selected transcripts (Table S2). Gene ontology (GO) classifications were

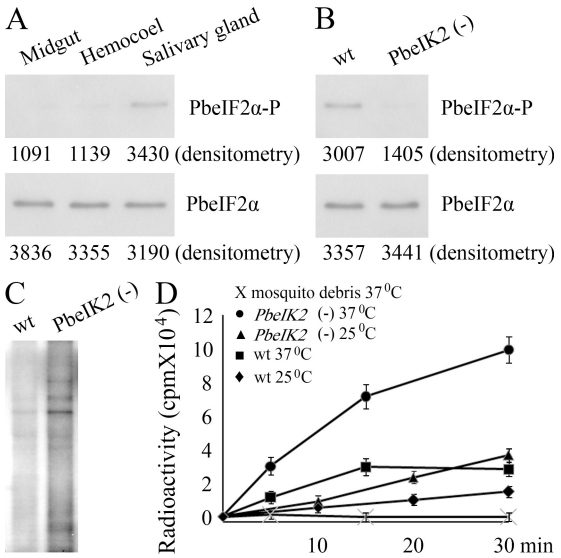

Figure 3. PbeIK2 leads to translational repression in salivary gland sporozoites. (A) 5 × 10^5 sporozoites of wild-type *P. berghei* were dissected from mosquito midguts, hemocoels, and salivary glands. Levels of PbeIF2α-P and total PbeIF2α were revealed by densitometry analysis of immunoblots. Values are shown below the bands. (B) PbeIF2α phosphorylation levels of wild-type and *PbeIK2* (-) salivary gland sporozoites were assayed by immunoblots. (C) The same number (5 × 10^5) of wild-type and *PbeIK2* (-) salivary gland sporozoites were exposed to ^{35}S-Met/Cys at 37°C for 30 min. Samples were then resolved on SDS-PAGE for autoradiography. (D) Effect of temperature on the kinetic incorporation of ^{35}S- Met/Cys by wild-type and *PbeIK2* (-) salivary gland sporozoites. These data were obtained in two independent experiments.

available for 21% (175) of the differentially expressed genes. Analysis showed that this group was strongly enriched for genes involved in translation at levels not expected by chance (P = 1.94e−7; Table II). This is likely to occur if, after the alleviation of repression, the translation machinery is expanded. In addition, we also noted that the genes showing the greatest up-regulation were the three mitochondrial-encoded enzymes, cytochrome c oxidase subunits 1 and III, and cytochrome b (Table S3). Mitochondrial proliferation is observed when sporozoites differentiate into early liver stages (Meis et al., 1985). Ubiquitin-like proteins, which are part of the proteasome system required for sporozoite remodelling and transformation into liver stages (Gantt et al., 1998), were also up-regulated (Table S3). Therefore, the global transcription analysis is consistent with the idea that mutants are beginning to transform into liver stages after dephosphorylation of eIF2α-P.

Further support for this idea was obtained by measuring the amounts of known liver stage proteins in wild type and mutants by Western blots. As shown in Fig. 5 A, HSP70 and UIS4 were increased in the *PbeIK2* (-) compared with wild type. HSP70 is barely detectable in sporozoites, but increased in liver stages (Tsuji et al., 1994; Kaiser et al. 2003). UIS4, a member of ETRAMP family, is transcribed but not translated in salivary gland sporozoites (Florens et al., 2002; Lasonder et al., 2008), and it localizes in the parasitophorous vacuole membrane surrounding the liver stages (Mueller et al. 2005). The amounts of the circumsporozoite protein (CSP), the major surface protein of sporozoites, associated with parasite extracts or secreted into the culture medium, were also increased in the mutant sporozoites (Fig. 5, A and B), even though the sporozoites have reduced gliding motility. In Western blots of salivary gland, sporozoites and the midgut sporozoites CSP appear as two bands (Yoshida et al., 1981), the lower one representing the proteolytically processing of the N terminus of CSP that is required for sporozoite invasion of hepatocytes (Coppi et al., 2005). As a control, in midgut sporozoites where *PbeIK2* is not transcribed, there was no difference in the levels of CSP associated with wild-type and *PbeIK2* (-) parasite extracts (Fig. 5 C).

eIF2α phosphorylation is controlled by a phosphatase

To test how eIF2α phosphorylation is regulated, wild-type sporozoites were incubated at 37°C, and the amounts of phosphorylated PbeIF2α were evaluated by Western blot analysis.

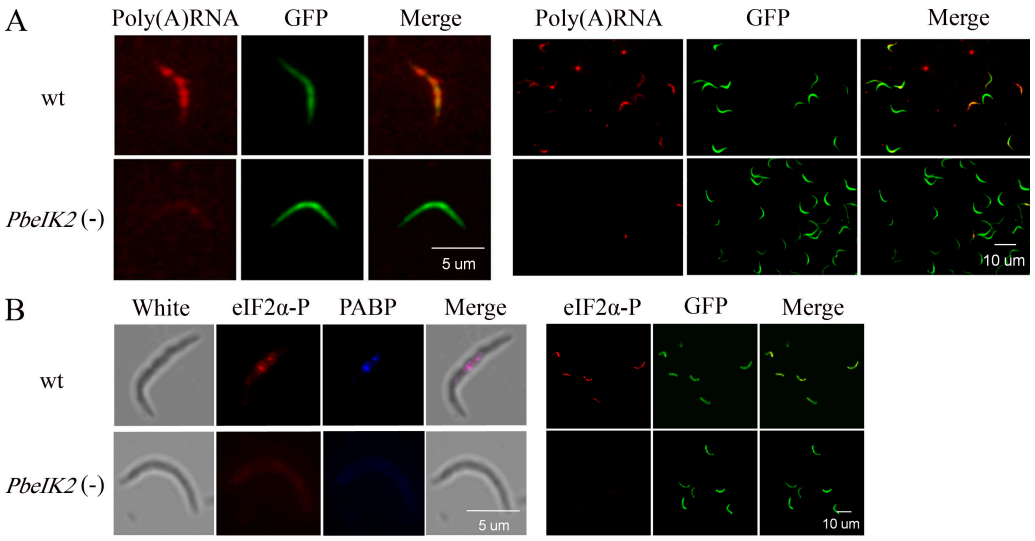

Figure 4. Stress granules in salivary gland sporozoites are PbeIK2 dependent. (A) The majority of wild-type salivary gland sporozoites contain poly(A) RNA granules. GFP-expressing sporozoites were subjected to oligo-d(T) in situ hybridization followed by fluorescence microscopy. (left) A higher magnification image. (B) Stress granule–associated proteins eIF2α-P and PABP were revealed by immunofluorescence in wild-type salivary gland sporozoites, but were absent in *PbeIK2* (-) sporozoites. (left) A higher magnification image. In situ hybridization and immunofluorescence assays were repeated in at least three independent experiments.

As shown in Fig. 6 A, dephosphorylation was noted between 30 and 60 min, which corresponds to the time when sporozoites lose infectivity. Salubrinal is a selective inhibitor of eIF2α dephosphorylation in mammalian cells (Boyce et al., 2005). As shown in Fig. 6 B, salivary gland sporozoite treatment with salubrinal increased the PbeIF2α phosphorylation levels in the wild type, but not in *PbeIK2* (-). Salubrinal treatment also significantly enhanced infectivity of wild-type sporozoites to HepG2 cells and to mice, but had no effect on the mutants (Fig. 6, C and D). Furthermore, the incorporation of radiolabeled amino acids in wild type, but not *PbeIK2* (-) sporozoites, was inhibited by salubrinal treatment (Fig. 6 E). We conclude that a phosphatase, not yet identified, modulates the eIF2α phosphorylation levels and therefore *Plasmodium* salivary gland sporozoites stage conversion.

Morphological changes in *PbeIK2* (-) sporozoites

The crescent-shaped sporozoite, typically upon invasion of a hepatocyte inside of a parasitophorous vacuole, progressively transforms into a spherical liver stage (Gantt et al., 1998).

Table II. Most significantly enriched GO categories in gene set regulated >2 fold in *PbeIK2* (-) compared to wild-type salivary gland sporozoites

GO accession no.	GO term	P-value	Count in selection	Count in selection	Count in total	Count in total
				%		%
GO:0010467	gene expression	0.0252	94	94.95	567	18.67
GO:0022626	cytosolic ribosome	0.0252	38	38.38	149	4.91
GO:0033279	ribosomal subunit	0.0373	42	42.42	178	5.86
GO:0022625	cytosolic large ribosomal subunit	0.0373	34	34.34	131	4.31
GO:0044445	cytosolic part	0.0393	40	40.40	177	5.83
GO:0015934	large ribosomal subunit	0.0393	37	37.37	151	4.97
GO:0022613	ribonucleoprotein complex biogenesis and assembly	0.0393	51	51.52	249	8.20
GO:0005840	ribosome	0.0433	48	48.48	224	7.38
GO:0005829	cytosol	0.0478	40	40.40	180	5.93
GO:0030529	ribonucleoprotein complex	0.0697	54	54.55	270	8.89
GO:0022618	ribonucleoprotein complex assembly	0.0743	45	45.45	217	7.15
GO:0006412	translation	0.0757	68	68.69	372	12.25
GO:0006413	translational initiation	0.0785	45	45.45	212	6.98

P-values were corrected for GO category dependencies. Microarray arrays data are the means of two wild-type salivary gland sporozoites and two *PbeIK2* (-) clones.

The pellicle of sporozoites is a triple membranous structure consisting of an inner membrane complex (IMC) made of flattened vesicles and placed underneath the plasma membrane. The sporozoite shape is maintained by microtubules lying longitudinally underneath the cytoplasmic side of the IMC (Khater et al., 2004). An actin-myosin motor used for motility and cell invasion is found between the plasma membrane and the IMC (Kappe et al., 2004). Shortly after sporozoites enter hepatocytes or are incubated at 37°C without host cells (Gantt et al., 1998; Kaiser et al., 2003), a characteristic "bulblike" structure (transformation bulb) appears in the body of the parasite. After a few hours, the parasite becomes spherical and the IMC disappears.

The morphology of *PbeIK2* (-) was examined by light microscopy and by transmission electron microscopy (TEM). By light microscopy, we documented the presence of the transformation bulbs in 3% of the *PbeIK2* (-) salivary gland sporozoites obtained immediately after dissection and fixation, whereas they were exceptionally seen in wild-type sporozoites (Fig. 7 A). After incubation at 37°C, the number of bulbs increased in a time-dependent fashion both in wild type and mutants. After a 4-h incubation, 52% of the *PbeIK2* (-) and 35% of wild-type sporozoites had bulbs detectable by light microscopy (Fig. 7 A). Notably, salubrinal treatment of wild-type salivary gland sporozoites significantly decreased the proportion of sporozoites displaying transformation bulbs after various incubation times at 37°C (Fig. 7 B). As previously reported, parasite remodeling was inhibited by MG132, a proteasome inhibitor (Gantt et al., 1998; Fig. 7 B). This is in agreement with the observation that transcripts encoding ubiquitin-like proteins were up-regulated in *PbeIK2* (-) (Table S3). TEM sections of the wild-type and mutant salivary gland sporozoites fixed immediately after collection revealed IMC disruption in the vicinity of the bulbs, plasma membrane detachment, and redistribution of organelles in mutant sporozoites (Fig. 7 C). In short, the morphological

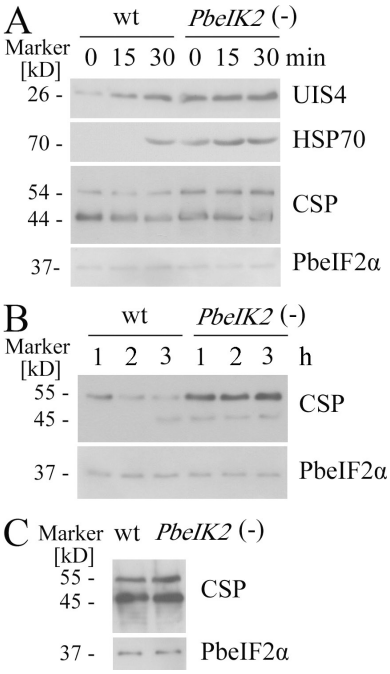

Figure 5. Enhanced liver stage proteins expression in *PbeIK2* (-) salivary gland sporozoites. (A) Wild-type and *PbeIK2* (-) sporozoites were incubated at 37°C for different times, then UIS4, HSP70, and CSP were visualized on immunoblots by using the polyclonal UIS4 antisera, mAb 2E6, and 3D11, respectively. Antiserum against total PbeIF2α served as loading controls. (B) Sporozoites were incubated at 25°C for different times, and the amounts of CSP secreted into the culture medium were immunoblotted with mAb 3D11. (C) CSP in wild-type and *PbeIK2* (-) midgut sporozoites. On day 14 after the first infectious blood meal, wild-type and *PbeIK2* (-) parasites were dissected from mosquito midguts, and CSP was visualized on immunoblot. Immunoblots were repeated at least three independent experiments.

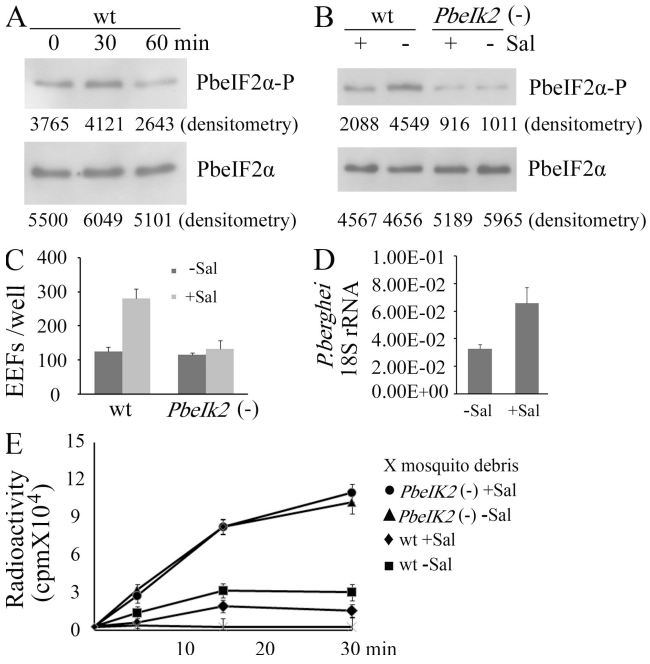

Figure 6. Evidence for the presence of a PbeIF2α phosphatase in salivary gland sporozoites. (A) Wild-type sporozoites were incubated at 37°C for 30 and 60 min, and then levels of PbeIF2α-P and total PbeIF2α were assayed by immunoblots. In B–E, wild-type and *PbeIK2* (-) sporozoites were dissected from mosquito salivary glands in the presence (+) or absence (-) of 1 uM salubrinal (Sal) at room temperature, and then the medium was replaced by DME supplemented with 10% FBS. (B) Immunoblot assays for levels of PbeIF2α-P and total PbeIF2α of wild-type and *PbeIK2* (-) sporozoites treated with or without Sal. In A and B, immunoblots were repeated at least four times and densitometry values are shown below bands. (C) Infectivity of Sal-treated sporozoites to HepG2 cells were evaluated by counting EEF numbers 48 h after infection. Data are shown as the means ± SD of three independent experiments. (D) Sal enhanced infectivity of wild-type sporozoites to mice. C57BL/6 mice (six mice per group) were intravenously injected with 5×10^3 wild-type sporozoites treated with or without Sal. 42 h later, liver parasite burden was measured by real-time PCR. Data are shown as the means ± SD of two independent experiments. (E) Effect of Sal on the kinetic incorporation of ^{35}S-Met/Cys by wild-type and *PbeIK2* (-) salivary gland sporozoites at 37°C. Data are shown as the means ± SD of two independent experiments.

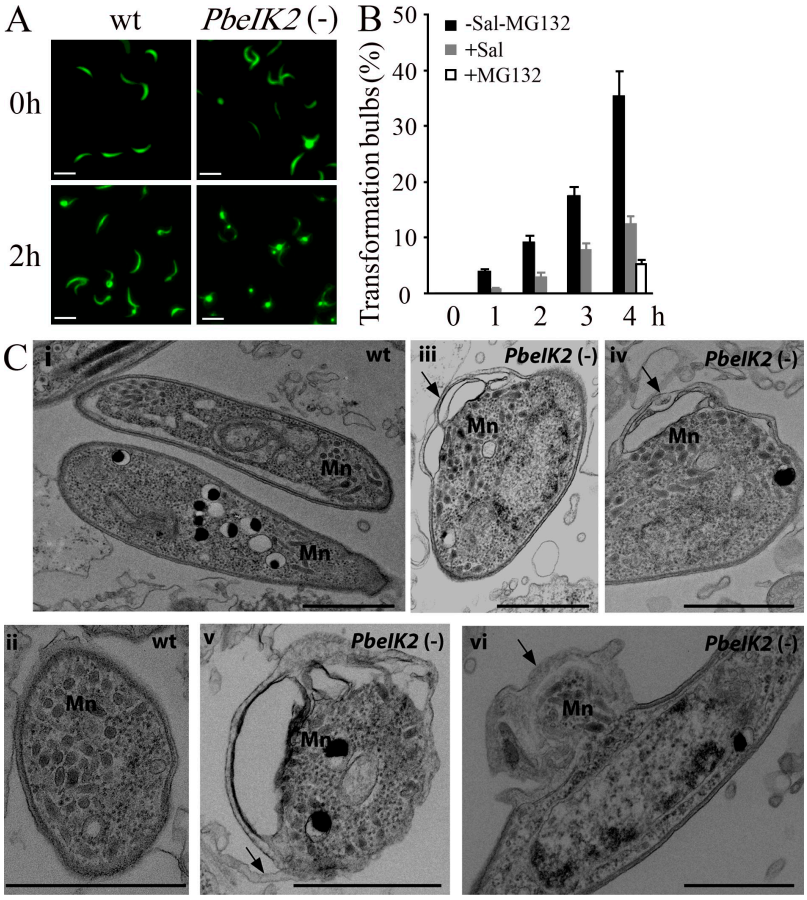

Figure 7. Morphology of *PbeIK2* (-) salivary gland sporozoites. (A) Fluorescence view of wild-type and *PbeIK2* (-) sporozoites fixed immediately after dissection from mosquito salivary glands or after 4 h incubation at 37°C. Bars, 10 µm. (B) Sal treated wild-type sporozoites were incubated at 37°C for different hours. Numbers of transformation bulbs were counted. One group of sporozoites was incubated with 50 µM proteasome inhibitor MG132 for 4 h. These data were obtained from two independent experiments. (C) TEM of *PbeIK2* (-) sporozoites fixed immediately after dissection from mosquito salivary glands. Mn, Micronemes. Panels i and ii, wild-type; iii-vi, mutant. Arrows in panels iii and iv point to bulbs; in panel v, membrane detachment; in panel vi, transformation bulb with redistribution of organelles. Bars, 1 µm.

changes that characterize the initial transformation of sporozoites into liver stages appear prematurely in the *PbeIK2* (-) salivary gland sporozoites.

DISCUSSION

The main finding of this paper is that *Plasmodium* salivary gland sporozoite latency and transformation into liver stages is dependent on the phosphorylation status of eIF2α, which is controlled by the IK2 kinase and by a phosphatase. IK2 activity is dominant in salivary gland sporozoites, leading to an inhibition of translation and accumulation of the stalled mRNAs into granules. When sporozoites are injected into the mammalian host, an eIF2α phosphatase removes the PO4 from eIF2α-P, and the repression of translation is alleviated to permit their transformation into liver stages. The IK2-mediated phosphorylation of eIF2α does not involve any obvious stress; instead, *IK2* is highly transcribed when midgut sporozoites enter the salivary glands of mosquitoes, as part of the normal *Plasmodium* life cycle. IK2 maintains the salivary gland sporozoites in a latent state before delivery into the host's skin. Thus, phosphorylation of eIF2α, which is used in mammalians cells in response to stress, regulates stage conversion in *Plasmodium*. The utilization of the mammalian stress–induced response by a protozoan parasite during its normal life cycle is not unique to *Plasmodium*. A case in point is the transformation of *Toxoplasma* tachyzoites into latent bradyzoites. Although the in vitro differentiation and phosphorylation of eIF2α is triggered by stress, bradyzoites also appear spontaneously during culture. The frequency of spontaneous change varies with the cultured cell type, the parasite strain, and other factors (Ferreira da Silva et al., 2008; Sullivan et al., 2009). The mechanisms of bradyzoite formation in vivo are unknown.

The primary function of *Plasmodium* IK2, like all mammalian eIF2α kinases, is to phosphorylate eIF2α and thereby inhibit protein synthesis. We document the presence of eIF2α-P in wild-type salivary gland sporozoites, but not in the control *PbeIK2* (-) or in midgut sporozoites, whose *IK2* is not transcribed (Fig. 3, A and B). The role of eIF2α phosphorylation in protein synthesis was studied by comparing the incorporation of radiolabeled amino acids in wild-type and mutant sporozoites. The global suppression of protein synthesis in wild-type sporozoites is illustrated in the radioautographs of the SDS-PAGEs (Fig. 3 C). We also measured the kinetics of incorporation in wild type and mutants at room temperature and at 37°C (Fig. 3 D). As shown, the rate of protein synthesis is much faster at the temperature of the mammalian host, and strikingly steeper in the mutant. Collectively these observations indicate that translation in wild-type salivary gland sporozoites is repressed. This is, indeed, the case shown by the presence of stress granules in the sporozoite's cytoplasm. We revealed the granules in wild-type salivary gland sporozoites by in situ hybridization of poly(A)$^+$ RNA, and by imaging with antibodies to components of the translation machinery that are found in stress granules, but not processing bodies (Fig. 4). The granules were absent in the *PbeIK2* (-) controls.

Our findings explain prior evidence that many transcripts accumulate in salivary gland sporozoites, but are not translated. For example, UIS4, LSAP-2, and LSAP-1 are among the most abundant transcripts in the salivary gland transcriptome (Le Roch et al., 2003), but have not been detected by proteomic surveys of liver stages (Florens et al., 2002;

Lasonder et al., 2008). In contrast, the abundant proteins in the salivary gland sporozoites CSP, TRAP, lactate dehydrogenase (PF13_0141), and phosphoglycerate kinase (PFI1105w) are translated from mRNAs in oocyst sporozoites (Zhou et al., 2008). Spearman rank calculations show a greater correlation between levels of proteins from salivary gland sporozoites and transcripts of oocyst sporozoites than between transcripts and proteins of the salivary gland (Table S4). There was a profound difference in the sets of transcribed genes between wild-type and *PbeIK2* (-) salivary gland sporozoites. Comparison of RNA arrays revealed that ~8% of the genes were up-regulated in the mutant, including many that are found predominantly in liver stages, such as mitochondrial and ubiquitin-like proteins. It is not known how this large burst of transcription is initiated, but perhaps one of the mRNAs that were silenced encodes transcription factor(s) for the set of liver stage genes.

The salivary gland sporozoites accumulate transcripts that will be needed in liver stages, but their translation is delayed until their transmission to the vertebrate host, when eIF2α-P is de-phosphorylated (Fig. 6 A). The relevant phosphatase has not been identified, but its presence in wild-type salivary gland sporozoites was revealed by using salubrinal, a specific inhibitor of the phosphatases that dephosphorylate eIF2α-P. Treatment of wild-type sporozoites with the drug enhanced phosphorylation of eIF2α and increased their infectivity in vitro and in vivo (Fig. 6). The interpretation of these results is that wild-type sporozoites bear both a kinase (IK2) and a phosphatase, but the activity of the kinase predominates in the salivary gland sporozoites; once the sporozoites enter the mammalian host, and/or during their migration to the liver, the phosphatase is activated and the translational repression is alleviated. In other words, when wild-type sporozoites are incubated at 37°C, their phenotype starts resembling that of the *PbeIK2* (-). This is the likely explanation for the well known phenomenon of the rapid loss of infectivity of sporozoites at 37°C (Vanderberg, 1974).

The transformation bulbs (Fig. 7 C) are associated with a localized disruption of the sporozoite's cytoskeleton that must impinge on the motility of the attached actin-myosin motor, leading to defects in gliding motility (Fig. S4 B), cell traversal (Fig. S4 A), and in turn to the profound inhibition of infectivity to mice (Table I). Bulb formation is prevented by a proteasome inhibitor, implying that these degradative machines are involved in the remodeling.

The in vitro infectivity of the mutants for HepG2 cells was indistinguishable from those of wild type (Fig. 2 E). The likely explanation for this apparent paradox is that the decreased motility of the *PbeIK2* (-) sporozoites was still adequate to promote the swift invasion of HepG2 cells. In vivo, however, the full activity of the sporozoite's actin myosin motor is required to cross skin cells and the sinusoidal barrier before hepatocyte invasion. This in vivo journey takes at least several minutes for wild-type sporozoites (Yamauchi et al., 2007), and is likely to be much longer in the mutants that are defective in cell traversal ability and gliding motility. It is during this journey that the loss of infectivity of the *PbeIK2* (-) takes place.

The complex life cycle of *Plasmodium* is highly regulated and involves a series of transcriptional changes and posttranscriptional modifications (Paton et al., 1993; Vervenne et al., 1994; Mair et al., 2010). As shown here, translational repression controlled by IK2 is an important mechanism to maintain infectivity of salivary gland sporozoites. The other two eIF2α kinases IK1 and PK4 are mostly transcribed in the asexual blood stages (Fig. 1). It is likely that the PK4 kinase, another member of the *Plasmodium* "stress" kinases, controls some essential step in the development of the asexual blood sages of *Plasmodium* because *PK4* cannot be disrupted. In another *Apicomplexan* parasite, *Toxoplasma*, eIF2α kinases initiate the in vitro transformation of tachyzoites into the latent cysts. Translational repression has been also well documented in *P. berghei* gametocytes (Thompson and Sinden, 1994) ingested by mosquitoes in whose stomachs fertilization and zygote formation takes place. The silent mRNAs accumulate in processing bodies that are stored in female gametocytes under the control of a conserved RNA helicase. In its absence, fertilization takes place, but the zygotes do not develop (Mair et al., 2010).

Finally, considering that arrest of translation is a frequent mechanism used by apicomplexa to achieve latency, it is not farfetched to speculate that an eIF2α kinase is involved in the generation of the still enigmatic dormant stages of the malaria parasite of humans, *P. vivax*.

MATERIALS AND METHODS

Transcription of PbeIF2α kinases. PbeIF2α kinases (PbeIK1, PB000582.03.0; PbeIK2, PB001255.02.0; PbPK4, PB000788.03.0) transcript levels were analyzed by real-time RT-PCR using cDNA prepared from asexual and mosquito-stage parasites of *P. berghei*. Real-time PCR was performed using iQ SYBR Green Supermix (Bio-Rad Laboratories), according to the manufacturer's instructions. The absence of genomic DNA contamination was confirmed by PCR amplification on same-treated RNA samples that lacked reverse transcription. The specificity of amplification for each PCR product was confirmed by dissociation curve analysis. Transcript expression was normalized to the expression of the control gene, arginyl-tRNA synthetase (PB000094.03.0). The normalized expression for each kinase was determined as the ratio: relative amount of target gene cDNA/relative amount of control gene cDNA. Gene-specific primers were arginyl-tRNA synthetase (sense 5′-TTGGTGATTGGGGAACAC-3′, antisense 5′-CTTGATATAAAAGGGTCAAAC-3′); PbeIK1 (sense 5′-TTCCGGTAACAACATCATG-3′, antisense 5′-CATGCATCATAATATCTCAC-3′); PbeIK2 (sense 5′-ATAGGTGATTTTGGTTTAGC-3′, antisense 5′-GTCACAGTTTTTATTTATTATCAG-3′); and PbPK4 (sense 5′-ATGGCAGATTTACGAGAAC-3′, antisense 5′-ATATGTTGGCGATCCTGGTTC-3′).

Generation of *PbeIK2* mutant parasites. For replacement of *PbeIK2* two fragments were amplified using PbeIK2rep5for (5′-CATTATATGGAAACAAAATACTTGTTAAAC-3′) and PbeIk2rep5rev (5′-ATTCGGTTCAACGTTGGTTAC-3′) for 500 base pair 5′ fragment, and PbeIK2rep3for (5′-TAGTCTTATCACAAATAATGGATATAT-3′) and PbeIK2rep3rev (5′-AAGTGAATAATAATAATATATATTATTAGTAC-3′) for 500 bp 3′ fragment using *P. berghei* genomic DNA as template. Details of double crossover replacement are described in Fig. S2.

Merozoites of *P. berghei* were transformed and *PbeIK2* mutant clones were selected as previously described (Janse et al., 2006).

Mosquito infection with *PbeIK2* mutant parasites. Animal care was in accordance with New York University School of Medicine laboratory animal protocol #071102. *Anopheles stephensi* mosquitoes were fed on anaesthetized Swiss Webster mice infected with wild-type parasites or with the *PbeIK2* (-) clones. 14 and 20 d after, the numbers of midgut and salivary gland sporozoites were counted.

Treatment of sporozoites. Sporozoites were dissected from mosquito salivary glands in RPMI medium, replaced by DME medium supplemented with 10% FBS (with or without 50 μM proteasome inhibitor MG132), and incubated at 37°C for different times. In some experiments, the dissection was made in medium containing 1 μM salubrinal.

Cell traversal ability. Hepa 1–6 cells were plated on 96-well plates and allowed to grow until subconfluent. They were loaded with 10 μM calcein blue (Invitrogen) for 1 h at 37°C and washed three times to remove unincorporated dye. 5×10^5 sporozoites were added to calcein blue–loaded cells. After incubation for 1 h at 37°C, supernatants containing the released calcein blue were transferred to a Microfluor 96-well plate (Thermo Fisher Scientific) and fluorescence was read in a Fluoroskan II (Labsystems) using excitation and emission wavelengths of 355 nm and 460 nm, respectively.

Gliding motility. Sporozoites were allowed to glide for 1 h at 37°C on Laboratory-Tek glass wells precoated with anti-CSP mAb 3D11 (Yoshida et al., 1980). Next, wells were fixed and stained with biotinylated mAb 3D11, followed by streptavidin-FITC to visualize the CSP-containing trails. Gliding motility was quantified by counting the number of circles in each trail.

Liver-stage parasite burden. To detect sporozoite infectivity in vitro, 1×10^5 HepG2 cell were seeded in eight-chamber slides and grown to semiconfluency. 2×10^4 or 2×10^3 Sporozoites were added, and liver stages were revealed after 48 h using antisera against parasitophorous vacuole membrane antigen UIS4 (Mueller et al., 2005). To detect liver stages in vivo 42 h after intravenous injection of sporozoites into C57BL/6 mice, the liver stage parasite burden was measured by real-time RT-PCR (Bruña-Romero et al., 2001). The normalized liver stage parasite burden was determined as the ratio: *P. berghei* 18S RNA copy number/mouse GAPDH copy number.

Sporozoite injection into droplets of medium. To study ejection of saliva and sporozoites by mosquitoes into RPMI medium, we used a modified method from a previous study (Kebaier et al., 2009). The feeding stylets of individual mosquitoes were immobilized on a microscope slide, and the mosquito was allowed to salivate into 5 μl of RPMI medium at room temperature for 10 min. The numbers of GFP fluorescent sporozoites released into the medium were counted by fluorescence microscopy.

Oligo-d(T) in situ hybridization. Oligo-d(T) in situ hybridization was performed as we previously described, except that 0.1% saponin was used instead of Triton X-100 (Chakraborty et al., 2006, 2008).

Immunofluorescence assay. Sporozoites were fixed on 12-well glass slides with 4% paraformaldehyde, permeabilized with chilled methanol, and immunostained with rabbit anti–eIF2α-P antibody (Narasimhan et al., 2008; 1:200 dilution) and mouse anti-PABP antibody (Tuteja and Pradhan, 2009; 1:200 dilution), at 37°C for 1 h. After three washes in PBS, slides were incubated with Alexa Fluor 594 goat anti–rabbit IgG and Alexa Fluor 350 goat anti–mouse IgG (1:500 dilution).

Microarray analysis. Total RNA from four samples of *P. berghei* salivary gland sporozoites (two wild-type controls and two *PbeIK2* mutant samples) was extracted with an RNeasy Mini kit (QIAGEN). Fragmented and biotin-labeled cDNA was synthesized from 100 ng total RNA according to the Affymetrix Two-Cycle Target Labeling protocol. Hybridization and scanning of the Affymetrix PlasmoFBa arrays were done according to the manufacturer's instructions (Affymetrix). Data were normalized using the quantile normalization method in RMA. Gene ontologies for *P. berghei* genes were downloaded from the gene ontology consortium. We calculated the probability of enrichment by chance for genes with a role in protein synthesis and translation in the group of genes showing a twofold change in the comparison between mutant and wild-type expression levels using Genespring software (Silicon Genetics). Microarray data are available at Gene Expression Omnibus database under accession no. GSE16259.

Comparison of protein and transcript levels. *P. falciparum* proteomic data for oocyst and salivary gland sporozoites were obtained from Lasonder et al. (2008) and *P. yoelii* transcription data from oocyst and salivary gland sporozoites was obtained from Zhou et al. (2008). 141 genes with an orthologue in both species, which contained >5 probes on the microarray and which were detected by more than five spectra in one of the two proteomic experiments were selected for comparison (Table S4).

Online supplemental material. Fig. S1 shows alignment of the catalytic subdomains of representative eIF2α kinase family members. Fig. S2 shows disruption of *PbeIK2* by double-crossover homologous recombination. Fig. S3 shows targeted disruption of the *PfeIK2* gene. Fig. S4 shows that *PbeIK2* (-) salivary gland sporozoites are defective in their ability to traverse cells and glide on glass slides. Table S1 shows *PfeIK2* is not required for infection of mosquitoes or progression through to sporozoites. Table S2 displays gene expression in *PbeIK2* (-) and wild-type salivary gland sporozoites by microarray and real-time RT-PCR. Table S3 displays mitochondrial genes, RNAs, and ubiquitin-like proteins up-regulated by more than two-fold in *PbeIK2* (-) compared with wild-type. Tab. S4 displays midgut and salivary gland sporozoites protein and transcript levels. Online supplemental material is available at http://www.jem.org/cgi/content/full/jem.20091975/DC1.

We thank Dr. David Ron for useful discussions and Tatiana Voza and Alida Coppi for parasitological technical support.

This work was supported in part by a grant from MMV and the Wellcome trust to the NGBS consortium to explore liver stage targets. E.A.W. is also supported by National Institutes of Health R01 AI059472 and by the Keck Foundation. V.N. is supported by the Bill and Melinda Gates Foundation, Dana Foundation and Novartis Foundation. W.J.S. is supported by a grant from the American Heart Association (AHA 0750201Z). S.M. is supported by Deutsche Forschungsgemeinschaft (ME 3528/1-1).

The authors have no conflicting financial interests.

Submitted: 11 September 2009
Accepted: 14 May 2010

REFERENCES

Balagopal, V., and R. Parker. 2009. Polysomes, P bodies and stress granules: states and fates of eukaryotic mRNAs. *Curr. Opin. Cell Biol.* 21:403–408. doi:10.1016/j.ceb.2009.03.005

Boyce, M., K.F. Bryant, C. Jousse, K. Long, H.P. Harding, D. Scheuner, R.J. Kaufman, D. Ma, D.M. Coen, D. Ron, and J. Yuan. 2005. A selective inhibitor of eIF2alpha dephosphorylation protects cells from ER stress. *Science.* 307:935–939. doi:10.1126/science.1101902

Boyd, M.F., W.K. Stratman-Thomas, and S.F. Kicthen. 1936. On the duration of infectiousness in anophelines harboring R falciparum. *Am. J. Trop. Med. Hyg.* 16:157–158.

Bruña-Romero, O., J.C. Hafalla, G. González-Aseguinolaza, G. Sano, M. Tsuji, and F. Zavala. 2001. Detection of malaria liver-stages in mice infected through the bite of a single Anopheles mosquito using a highly sensitive real-time PCR. *Int. J. Parasitol.* 31:1499–1502. doi:10.1016/S0020-7519(01)00265-X

Chakraborty, P., N. Satterly, and B.M. Fontoura. 2006. Nuclear export assays for poly(A) RNAs. *Methods.* 39:363–369. doi:10.1016/j.ymeth.2006.07.002

Chakraborty, P., Y. Wang, J.H. Wei, J. van Deursen, H. Yu, L. Malureanu, M. Dasso, D.J. Forbes, D.E. Levy, J. Seemann, and B.M. Fontoura. 2008. Nucleoporin levels regulate cell cycle progression and phase-specific gene expression. *Dev. Cell*. 15:657–667. doi:10.1016/j.devcel.2008.08.020

Coppi, A., C. Pinzon-Ortiz, C. Hutter, and P. Sinnis. 2005. The *Plasmodium* circumsporozoite protein is proteolytically processed during cell invasion. *J. Exp. Med*. 201:27–33. doi:10.1084/jem.20040989

Dar, A.C., T.E. Dever, and F. Sicheri. 2005. Higher-order substrate recognition of eIF2alpha by the RNA-dependent protein kinase PKR. *Cell*. 122:887–900. doi:10.1016/j.cell.2005.06.044

Fennell, C., S. Babbitt, I. Russo, J. Wilkes, L. Ranford-Cartwright, D.E. Goldberg, and C. Doerig. 2009. PfeIK1, a eukaryotic initiation factor 2alpha kinase of the human malaria parasite *Plasmodium falciparum*, regulates stress-response to amino-acid starvation. *Malar. J.* 8:99. doi:10.1186/1475-2875-8-99

Ferreira da Silva, Mda.F., H.S. Barbosa, U. Gross, and C.G. Lüder. 2008. Stress-related and spontaneous stage differentiation of Toxoplasma gondii. *Mol. Biosyst*. 4:824–834. doi:10.1039/b800520f

Florens, L., M.P. Washburn, J.D. Raine, R.M. Anthony, M. Grainger, J.D. Haynes, J.K. Moch, N. Muster, J.B. Sacci, D.L. Tabb, et al. 2002. A proteomic view of the *Plasmodium falciparum* life cycle. *Nature*. 419:520–526. doi:10.1038/nature01107

Gantt, S.M., J.M. Myung, M.R. Briones, W.D. Li, E.J. Corey, S. Omura, V. Nussenzweig, and P. Sinnis. 1998. Proteasome inhibitors block development of *Plasmodium* spp. *Antimicrob. Agents Chemother.* 42:2731–2738.

Janse, C.J., J. Ramesar, and A.P. Waters. 2006. High-efficiency transfection and drug selection of genetically transformed blood stages of the rodent malaria parasite *Plasmodium berghei*. *Nat. Protoc*. 1:346–356. doi:10.1038/nprot.2006.53

Kaiser, K., N. Camargo, and S.H. Kappe. 2003. Transformation of sporozoites into early exoerythrocytic malaria parasites does not require host cells. *J. Exp. Med*. 197:1045–1050. doi:10.1084/jem.20022100

Kappe, S.H., C.A. Buscaglia, and V. Nussenzweig. 2004. *Plasmodium* sporozoite molecular cell biology. *Annu. Rev. Cell Dev. Biol*. 20:29–59. doi:10.1146/annurev.cellbio.20.011603.150935

Kebaier, C., T. Voza, and J. Vanderberg. 2009. Kinetics of mosquito-injected *Plasmodium* sporozoites in mice: fewer sporozoites are injected into sporozoite-immunized mice. *PLoS Pathog*. 5:e1000399. doi:10.1371/journal.ppat.1000399

Kedersha, N., and P. Anderson. 2007. Mammalian stress granules and processing bodies. *Methods Enzymol*. 431:61–81. doi:10.1016/S0076-6879(07)31005-7

Khater, E.I., R.E. Sinden, and J.T. Dessens. 2004. A malaria membrane skeletal protein is essential for normal morphogenesis, motility, and infectivity of sporozoites. *J. Cell Biol*. 167:425–432. doi:10.1083/jcb.200406068

Lasonder, E., C.J. Janse, G.J. van Gemert, G.R. Mair, A.M. Vermunt, B.G. Douradinha, V. van Noort, M.A. Huynen, A.J. Luty, H. Kroeze, et al. 2008. Proteomic profiling of *Plasmodium* sporozoite maturation identifies new proteins essential for parasite development and infectivity. *PLoS Pathog*. 4:e1000195. doi:10.1371/journal.ppat.1000195

Le Roch, K.G., Y. Zhou, P.L. Blair, M. Grainger, J.K. Moch, J.D. Haynes, P. De La Vega, A.A. Holder, S. Batalov, D.J. Carucci, and E.A. Winzeler. 2003. Discovery of gene function by expression profiling of the malaria parasite life cycle. *Science*. 301:1503–1508. doi:10.1126/science.1087025

Mair, G.R., E. Lasonder, L.S. Garver, B.M. Franke-Fayard, C.K. Carret, J.C. Wiegant, R.W. Dirks, G. Dimopoulos, C.J. Janse, and A.P. Waters. 2010. Universal features of post-transcriptional gene regulation are critical for *Plasmodium* zygote development. *PLoS Pathog*. 6:e1000767. doi:10.1371/journal.ppat.1000767

Meis, J.F., J.P. Verhave, P.H. Jap, and J.H. Meuwissen. 1985. Transformation of sporozoites of *Plasmodium berghei* into exoerythrocytic forms in the liver of its mammalian host. *Cell Tissue Res*. 241:353–360. doi:10.1007/BF00217180

Mota, M.M., G. Pradel, J.P. Vanderberg, J.C. Hafalla, U. Frevert, R.S. Nussenzweig, V. Nussenzweig, and A. Rodríguez. 2001. Migration of *Plasmodium* sporozoites through cells before infection. *Science*. 291:141–144. doi:10.1126/science.291.5501.141

Mueller, A.K., N. Camargo, K. Kaiser, C. Andorfer, U. Frevert, K. Matuschewski, and S.H. Kappe. 2005. *Plasmodium* liver stage developmental arrest by depletion of a protein at the parasite-host interface. *Proc. Natl. Acad. Sci. USA*. 102:3022–3027. doi:10.1073/pnas.0408442102

Narasimhan, J., B.R. Joyce, A. Naguleswaran, A.T. Smith, M.R. Livingston, S.E. Dixon, I. Coppens, R.C. Wek, and W.J. Sullivan Jr. 2008. Translation regulation by eukaryotic initiation factor-2 kinases in the development of latent cysts in *Toxoplasma gondii*. *J. Biol. Chem*. 283:16591–16601. doi:10.1074/jbc.M800681200

Paton, M.G., G.C. Barker, H. Matsuoka, J. Ramesar, C.J. Janse, A.P. Waters, and R.E. Sinden. 1993. Structure and expression of a post-transcriptionally regulated malaria gene encoding a surface protein from the sexual stages of *Plasmodium berghei*. *Mol. Biochem. Parasitol*. 59:263–275. doi:10.1016/0166-6851(93)90224-L

Porter, R.J., R.L. Laird, and E.M. Dusseau. 1954. Studies on malarial sporozoites. II. Effect of age and dosage of sporozoites on their infectiousness. *Exp. Parasitol.* 3:267–274. doi:10.1016/0014-4894(54)90026-0

Proud, C.G. 2005. eIF2 and the control of cell physiology. *Semin. Cell Dev. Biol*. 16:3–12. doi:10.1016/j.semcdb.2004.11.004

Sherman, I.W. 1998. Malaria: Parasite Biology, Pathogenesis, and Protection. American Society for Microbiology, Washington, DC. 56 pp.

Sullivan, W.J. Jr., J. Narasimhan, M.M. Bhatti, and R.C. Wek. 2004. Parasite-specific eIF2 (eukaryotic initiation factor-2) kinase required for stress-induced translation control. *Biochem. J.* 380:523–531. doi:10.1042/BJ20040262

Sullivan, W.J. Jr., A.T. Smith, and B.R. Joyce. 2009. Understanding mechanisms and the role of differentiation in pathogenesis of *Toxoplasma gondii*: a review. *Mem. Inst. Oswaldo Cruz*. 104:155–161.

Thompson, J., and R.E. Sinden. 1994. In situ detection of Pbs21 mRNA during sexual development of *Plasmodium berghei*. *Mol. Biochem. Parasitol*. 68:189–196. doi:10.1016/0166-6851(94)90164-3

Tsuji, M., D. Mattei, R.S. Nussenzweig, D. Eichinger, and F. Zavala. 1994. Demonstration of heat-shock protein 70 in the sporozoite stage of malaria parasites. *Parasitol. Res*. 80:16–21. doi:10.1007/BF00932618

Tuteja, R., and A. Pradhan. 2009. Isolation and functional characterization of eIF4F components and poly(A)-binding protein from *Plasmodium falciparum*. *Parasitol. Int*. 58:481–485. doi:10.1016/j.parint.2009.09.001

Van Der Kelen, K., R. Beyaert, D. Inzé, and L. De Veylder. 2009. Translational control of eukaryotic gene expression. *Crit. Rev. Biochem. Mol. Biol*. 44:143–168. doi:10.1080/10409230902882090

Vanderberg, J.P. 1974. Studies on the motility of *Plasmodium* sporozoites. *J. Protozool*. 21:527–537.

Vervenne, R.A., R.W. Dirks, J. Ramesar, A.P. Waters, and C.J. Janse. 1994. Differential expression in blood stages of the gene coding for the 21-kilodalton surface protein of ookinetes of *Plasmodium berghei* as detected by RNA in situ hybridisation. *Mol. Biochem. Parasitol*. 68:259–266. doi:10.1016/0166-6851(94)90170-8

Ward, P., L. Equinet, J. Packer, and C. Doerig. 2004. Protein kinases of the human malaria parasite *Plasmodium falciparum*: the kinome of a divergent eukaryote. *BMC Genomics*. 5:79. doi:10.1186/1471-2164-5-79

Yamauchi, L.M., A. Coppi, G. Snounou, and P. Sinnis. 2007. Plasmodium sporozoites trickle out of the injection site. *Cell. Microbiol*. 9:1215–1222. doi:10.1111/j.1462-5822.2006.00861.x

Yoshida, N., R.S. Nussenzweig, P. Potocnjak, V. Nussenzweig, and M. Aikawa. 1980. Hybridoma produces protective antibodies directed against the sporozoite stage of malaria parasite. *Science*. 207:71–73. doi:10.1126/science.6985745

Yoshida, N., P. Potocnjak, V. Nussenzweig, and R.S. Nussenzweig. 1981. Biosynthesis of Pb44, the protective antigen of sporozoites of *Plasmodium berghei*. *J. Exp. Med*. 154:1225–1236. doi:10.1084/jem.154.4.1225

Zhou, Y., V. Ramachandran, K.A. Kumar, S. Westenberger, P. Refour, B. Zhou, F. Li, J.A. Young, K. Chen, D. Plouffe, et al. 2008. Evidence-based annotation of the malaria parasite's genome using comparative expression profiling. *PLoS One*. 3:e1570. doi:10.1371/journal.pone.0001570